Synthesis and Spectroscopic Characterization of Model Compounds for the Active Site Cofactor in Copper Amine Oxidases[†,‡]

Minae Mure and Judith P. Klinman*

Contribution from the Department of Chemistry, University of California, Berkeley, California 94720

Received January 26, 1993

Abstract: The synthesis and spectroscopic characterization of compounds which model different forms of the active site cofactor in copper amine oxidases have been pursued. As described, 5-(2,4,5-trihydroxybenzyl)hydantoin ($\mathbf{1}_{red}H_3$), its corresponding quinone ($\mathbf{1}_{ox}H$), and 6-amino-4-ethylresorcinol ($\mathbf{7}H_2$) have been prepared. Additionally, 5-(3,4-dihydroxybenzyl)hydantoin ($\mathbf{2}_{red}H_2$) was synthesized for comparative purposes. Spectroscopic titrations have been employed to determine the pK_a values of the acid–base species of the quinone ($\mathbf{A} = \mathbf{1}_{ox}H + \mathbf{1}_{ox}^-$; eq 3), the quinol ($\mathbf{B} = \mathbf{1}_{red}H_3 + \mathbf{1}_{red}H_2^- + \mathbf{1}_{red}H^{2-} + \mathbf{1}_{red}^{3-}$; eq 2), and the aminophenol ($\mathbf{C} = \mathbf{7}H_3^+ + \mathbf{7}H_2 + \mathbf{7}H^- + \mathbf{7}^{2-}$; eq 4). The quinone ($\mathbf{1}_{ox}H$) has a p$K_a$ of 4.13 ± 0.01. The anionic species ($\mathbf{1}_{ox}^-$) has a broad absorption band at around 484 nm which is characteristic of the eukaryotic copper amine oxidases. The quinol (B) and the aminophenol (C) have no absorption in this region, comparable to the reduced forms of enzymes. At pH 7.20, the two-electron redox potential of topa quinone ($\mathbf{1}_{ox}^-$) is shown to be ca. 300 mV less positive than that of dopa quinone ($\mathbf{2}_{ox}$) but to be similar to that of pyrroloquinoline quinone (PQQ). The aminophenol ($\mathbf{C}' = \mathbf{7}H_2 + \mathbf{7}H^- + \mathbf{7}^{2-}$) and the quinol (B) have similar acid–base properties and electrochemistry at neutral and basic conditions. The iminoquinone (**9**) is easily generated by oxidation of the aminophenol (C′) exhibiting a blue-shifted λ_{max} which is similar to that observed in a complex of a copper amine oxidase and ammonia. (4-Nitrophenyl)hydrazine readily forms the hydrazone (azo) of $\mathbf{1}_{ox}H$ (**3**). The position of the nucleophilic addition is shown by 2D NMR experiments to be at C5, the carbonyl carbon next to the hydroxyl group.

Introduction

Eukaryotic copper-containing amine oxidases (EC 1.4.3.6) catalyze a two-electron ($2e^-$) oxidative deamination of primary amines concomitant with reduction of dioxygen to hydrogen peroxide (eq 1).[1] In addition to active site copper, these enzymes

$$RCH_2NH_2 + O_2 + H_2O \rightarrow RCHO + NH_3 + H_2O_2 \quad (1)$$

contain a covalently bound organic cofactor which has a carbonyl group capable of forming a chromophoric complex with phenylhydrazine. The nature of the cofactor has been the subject of much controversy. In 1984, pyrroloquinoline quinone (PQQ) or a closely similar compound was proposed to be the organic cofactor.[2] However, recent studies clearly show that the active site cofactor of bovine serum amine oxidase (BSAO) is 6-hydroxydopa (topa).[3]

The identification of the cofactor has been achieved by derivatization of the enzyme-bound cofactor with phenylhydrazine or 4-nitrophenylhydrazine to form a stable hydrazine adduct, followed by spectroscopic characterization of intact protein derivatives[4] or active site derived cofactor-containing peptides.[3,4,5] In addition to BSAO, amine oxidases isolated from yeast,[5] porcine and sheep plasma, porcine kidney, and pea and chick pea seedlings[4] are demonstrated to contain topa quinone as the redox active cofactor.

We have used topa hydantoin quinone ($\mathbf{1}_{ox}H$) as a model compound of the covalently bound cofactor. In this paper, we have described the synthesis of $\mathbf{1}_{ox}H$, its corresponding quinol $\mathbf{1}_{red}H_3$, the aminophenol $\mathbf{7}H_2$, and dopa hydantoin ($\mathbf{2}_{red}H_2$) and characterized their acid–base properties and electrochemistry. The (4-nitrophenyl)hydrazone derivative of $\mathbf{1}_{ox}H$ (**3**) has also been prepared and its structure assigned by 2D NMR experiments. Results of these studies provide important insight into the mechanistic properties of topa at the active site of copper amine oxidases.

Experimental Procedures

Materials. 2,4,5-Tribenzyloxybenzaldehyde was obtained from Regis, 3,4-dibenzyloxybenzaldehyde was from Aldrich, and sodium amalgam was from Anachemia. All other chemicals were reagent grade and were obtained from either Aldrich or Sigma. Bovine serum amine oxidase (BSAO) was purified according to the method previously described.[6] The purified enzyme had a specific activity of 0.33 units/mg of protein; 1 unit is defined as the amount of enzyme which catalyzes the production of 1 μmol of benzaldehyde/min when 10 mM benzylamine is employed as substrate in 100 mM phosphate buffer, pH 7.2. Protein concentration was determined using a kit from Bio-Rad with bovine serum albumin as the protein standard.

Synthesis of 5-(2,4,5-Tribenzyloxybenzylidine)hydantoin.[7] 2,4,5-Tribenzyloxybenzaldehyde (29.4 mmol, 12.5 g) was slowly added to a stirred mixture of hydantoin (64 mmol, 6.4 g) and sodium acetate (78 mmol, 6.4 g) in 16 mL of glacial acetic acid and 1 mL of acetic anhydride at 100 °C in a three-necked round-bottomed flask equipped with a thermometer. After the addition was complete, the reaction was refluxed for 3.5 h, during which the internal temperature increased from 150 to 160 °C. The hot, viscous reaction mixture was poured into a 1-L heavy-walled beaker and slowly cooled, yielding a crystalline mass covered with a thin layer of red material, which was removed by rinsing with copious

† Supported by a grant from the National Institutes of Health (GM 39296).

‡ Abbreviations: PQQ, pyrroloquinoline quinone; BSAO, bovine serum amine oxidase; HRMS, high resolution mass spectroscopy; ROESY, rotating-frame Overhauser and exchange spectroscopy; HMQC, heteronuclear multiple-quantum correlation; HMBC, heteronuclear multiple-bond correlation; TPPI, time proportional phase incrementation; CV, cyclic voltammetry.

* To whom correspondence should be addressed.

(1) *Structure and Functions of Amine Oxidases*; Mondovi, B., Ed.; CRC Press: Boca Raton, FL, 1985.

(2) (a) Ameyama, M.; Hayashi, M.; Matsushita, K.; Shinagawa, E.; Adachi, O. *Agric. Biol. Chem.* **1984**, *48*, 561–565. (b) Lobenstein-Verbeek, C. L.; Jongejan, J. A.; Frank, J.; Duine, J. A. *FEBS Lett.* **1984**, *48*, 561–565.

(3) Janes, S. M.; Mu, D.; Wemmer, D.; Smith, A. J.; Kaur, S.; Maltby, D.; Burlingame, A. L.; Klinman, J. P. *Science* **1990**, *248*, 981–987.

(4) Janes, S. M.; Palcic, M. M.; Scaman, C. H.; Smith, A. J.; Brown, D. E.; Dooley, D. M.; Mure, M.; Klinman, J. P. *Biochemistry* **1992**, *31*, 12147–12154.

(5) Mu, D.; Janes, S. M.; Smith, A. J.; Brown, D. E.; Dooley, D. M.; Klinman, J. P. *J. Biol. Chem.* **1992**, *267*, 7979–7982.

(6) Janes, S. M.; Klinman, J. P. *Biochemistry* **1991**, *30*, 4599–4605.

(7) Janes, S. M. Ph.D. Thesis, University of California, Berkeley, 1990.

0002-7863/93/1515-7117$04.00/0

amounts of water and then several times with a small amount of cold ethanol. The remaining solid was recrystallized from chloroform to yield 5-(2,4,5-tribenzyloxybenzylidine)hydantoin (6.95 g, 54%) as yellow needles: mp 189–190 °C; TLC (silica) R_f = 0.67 (chloroform); MS m/e 506 (M^+); ^{1}H NMR (acetone-d_6) δ 5.15 (2H, s), 5.19 (2H, s), 5.22 (2H, s), 6.74 (1H, s), 7.02 (1H, s), 7.28 (1H, s), 7.4 (15H, m). Anal. Calcd for $C_{31}H_{26}N_2O_5$: C, 73.5; H, 5.1; N, 5.5 Found: C, 73.61; H, 4.80; N, 5.14.

Synthesis of 5-(2,4,5-Tribenzyloxybenzyl)hydantoin.[7] Sodium amalgam (3% w/w, 100 g) was added over 15 min to a stirred suspension of 5-(2,4,5-tribenzyloxybenzylidine)hydantoin (9 g, 18 mmol) in dioxane/water (130 mL/20 mL). The reaction was vigorously stirred until the color changed to pale yellow (ca. 12 h). The solution was decanted from sodium amalgam, diluted with 100 mL of water, cooled on ice, and acidified to pH 6.5 with HCl. The precipitated product was extracted with ethyl acetate, dried with $MgSO_4$, and concentrated under reduced pressure to give a yellow oil. A solid was obtained after treatment with benzene and hexane, which recrystallized from acetone/H_2O to give 5-(2,4,5-tribenzyloxybenzyl)hydantoin (7 g, 77%) as white needles: mp 177–178 °C; TLC (silica) R_f = 0.8 (ethyl acetate/petroleum ether, 9/1); MS, m/e 508 (M^+); ^{1}H NMR (acetone-d_6) δ 2.73 (1H, dd), 3.29 (1H, dd), 4.36 (1H, dd), 5.06 (2H, s), 5.12 (2H, s), 5.14 (2H, s), 6.92 (1H, s), 7.00 (1H, s), 7.4 (15H, m). Anal. Calcd for $C_{31}H_{28}N_2O_5$: C, 73.2; H, 5.5; N, 5.5. Found: C, 72.91; H, 5.25; N, 5.42.

Synthesis of 5-(2,4,5-Trihydroxybenzyl)hydantoin ($1_{red}H_3$). A suspension of 5-(2,4,5-tribenzyloxybenzyl)hydantoin (200 mg, 0.4 mmol) and palladized charcoal (5%) in 13 mL of 95% ethanol containing 3 drops of 3.0 N HCl was hydrogenated at 45 psi in a Parr apparatus for 5 h. The catalyst was removed by filtration and rinsed with a small portion of acidic ethanol several times in an Ar atmosphere. The solvent was removed under vacuum, and the remaining solid was washed with ether several times and dried under vacuum to give 5-(2,4,5-trihydroxybenzyl)hydantoin ($1_{red}H_3$) as a white solid (82.5 mg, 87%): HRMS, for $C_{10}H_{11}N_2O_5$ (MH^+), calcd m/z 239.0668, obsd m/z 239.0666; ^{1}H NMR (DMSO-d_6) δ 2.46 (dd, 1H, J = 13.8, 7.5 Hz), 2.90 (dd, 1H, J = 13.8, 4.7 Hz), 4.14 (dd, 1H, J = 7.5, 4.7 Hz), 6.28 (s, 1H), 6.42 (s, 1H), 7.59 (s, 1H, exchangeable with D_2O), 8.03 (br s, exchangeable with D_2O), 8.57 (s, 1H, exchangeable with D_2O), 8.61 (br s, exchangeable with D_2O), 10.49 (s, 1H, exchangeable with D_2O).

Synthesis of 2-Hydroxy-5-(5′-hydantoinmethyl)-1,4-benzoquinone ($1_{ox}H$). A 100-mg (0.42 mmol) sample of 5-(2,4,5-trihydroxybenzyl)-hydantoin ($1_{red}H_3$) was oxidized to the quinone with a catalytic amount of triethylamine in 10 mL of dry methanol. The reaction was stirred for 1 h, and the solvent was removed by rotary evaporation. The remaining sample was purified on a silica gel column. First, the small amount of the quinone ($1_{ox}H$) was eluted with ethanol (a pale yellow fraction). The deprotonated form of the quinone (1_{ox}^-) was then eluted as a Na^+ salt (Na^+ is the counterion in neutral silica gel) with ethanol/methanol (5/2, v/v) (a red fraction). Total yield was 91%. $1_{ox}H$: MS, m/e 238 (M^+ + 2); ^{1}H NMR (DMSO-d_6) δ 2.46 (dd, 1H, J = 13.58, 9.10 Hz), 2.83 (dd, 1H, J = 13.58, 4.64 Hz), 4.15 (dd, 1H, J = 9.10, 4.63 Hz), 6.07 (s, 1H, exchangeable with DCl), 6.63 (s, 1H), 8.00 (br s, exchangeable with D_2O), 10.73 (br s, exchangeable with D_2O); UV λ_{max} 350 nm (MeOH). $1_{ox}^-Na^+$: MS, Na^+ suppressed the product peaks; ^{1}H NMR (DMSO-d_6) δ 2.32 (dd, 1H, J = 13.52, 9.01 Hz), 2.85 (dd, 1H, J = 13.52, 4.51 Hz), 4.18 (dd, 1H, J = 9.01, 4.51 Hz), 5.00 (s, 1H, exchangeable with D_2O), 6.11 (s, 1H), 7.93 (s, 1H, exchangeable with D_2O), 10.62 (s, 1H, exchangeable with D_2O); ^{13}C NMR (DMSO-d_6) δ 31.54, 56.39, 108.71, 132.37, 144.08, 157.16, 174.94, 175.79, 183.68.

Oxidation of $1_{red}H_3$ by $NaIO_4$. $1_{red}H_3$ (40 mg, 0.17 mmol) was dissolved in methanol (10 mL) and was reacted with a 3 M excess of $NaIO_4$ (72.8 mg, 0.3 mmol) for 1 h. The catalyst was removed by centrifugation. The solvent was removed by rotary evaporation, and the remaining sample was purified on a silica gel column. The purple colored fraction was eluted with ethylacetate/ethanol (5/2, v/v) (total yield was 14.0 mg (35%)): MS, m/e 237 (M^+ + 1); ^{1}H NMR (DMSO-d_6) δ 2.41 (dd, 1H, J = 13.3, 9.5 Hz), 2.94 (dd, 1H, J = 13.3, 4.2 Hz), 4.2 (dd, 1H, J = 9.5, 4.2 Hz), 6.16 (s, 1H), 7.97 (s, 1H, exchangeable with D_2O), 10.64 (s, 1H, exchangeable with D_2O); ^{13}C NMR (DMSO-d_6) δ 33.94, 56.81, 79.87, 128.74, 147.89, 157.28, 169.38, 175.19, 177.11, 185.04; UV λ_{max} 261, 440 nm (pH 1.67), λ_{max} 270, 524 nm (pH 5.63); pK_a = 2.42.

Synthesis of 4-Ethyl-6-nitrosoresorcinol (6). A 1.518-g (0.022 mol) sample of $NaNO_2$ in 8.4 mL of H_2O was added dropwise to a stirred and cooled (−5 to 5 °C) solution of 3 g (0.022 mol) of 4-ethylresorcinol (Aldrich) in 77 mL of 95% ethanol containing a 10 M excess of HCl. After 15 min, an orange-red solid was precipitated. The solid was separated off by filtration, washed with a small portion of cold ethanol, and dried in vacuo to give 3.02 g of 4-ethyl-6-nitrosoresorcinol (82% yield): MS, m/e 168 (M^+ + 1); ^{1}H NMR (DMSO-d_6) δ 1.0 (t, 3H, J = 7.75 Hz), 2.30 (q, 2H, J = 7.75 Hz), 5.70 (s, 1H, exchangeable with D_2O), 7.33 (s, 1H); ^{1}H NMR ($CDCl_3$) δ 1.218 (t, 3H, J = 7.55 Hz), 2.570 (q, 2H, J = 7.55 Hz), 6.43 (s, 1H), 7.88 (s, 1H).

Synthesis of 6-Amino-4-ethylresorcinol ($7H_2$). 4-Ethyl-6-nitrosoresorcinol (200 mg) was added in small portions to a solution of $SnCl_2 \cdot 2H_2O$ (0.933 g) in concentrated HCl (5 mL). The mixture was vigorously stirred at 60–70 °C for 5 h. After complete removal of solvent, greenish white solids were obtained under anaerobic conditions. The solids were dissolved in a small amount of degassed water, and then H_2S gas was bubbled through until all the Sn^{2+} was converted to SnS. The solution was kept under an H_2S atmosphere for 1 day. SnS was removed by filtration and washed with HCl(aq) several times. The filtrate and the HCl solution were combined and concentrated under anaerobic conditions. 6-Amino-4-ethylresorcinol ($7H_2$) was obtained as a colorless crystalline needle HCl salt after cooling (in 69% yield): MS, m/e 154 (M^+ − Cl), 137 (154 − NH_3); ^{1}H NMR ($CDCl_3$ + DMSO-d_6) δ 1.114 (t, 3H, J = 7.40 Hz), 2.475 (q, 2H, J = 7.40 Hz), 6.694 (s, 1H), 7.032 (s, 1H), 9.235 (br s, 1H, exchangeable with D_2O), 9.571 (br s, 2H, exchangeable with D_2O), 9.936 (br s, 1H, exchangeable with D_2O). Anal. Calcd for $C_8H_{12}NO_2Cl \cdot {}^1/_2H_2O$: C, 48.37; H, 6.59; N, 7.05. Found: C, 48.11; H, 6.50; N, 6.76.

Synthesis of a 4-Nitrophenylhydrazone Derivative of 2-Hydroxy-5-(5′-hydantoinmethyl)-1,4-benzoquinone (3). The quinone (1_{ox}^-) was generated by air oxidation of the quinol in the presence of a catalytic amount of triethylamine in dry methanol. An excess amount (20 equiv) of (4-nitrophenyl)hydrazine hydrochloride was added to the solution. After 1 h, orange-red precipitates were collected by centrifugation and washed with a small portion of acetone several times. The supernatant was treated with ether, and the excess (4-nitrophenyl)hydrazine hydrochloride was removed by centrifugation. The ether and acetone solutions were combined and concentrated under reduced pressure to give an orange-red oil. The oil was purified by silica gel chromatography. The (4-nitrophenyl)hydrazone adduct (3) was eluted by acetone (total yield was 32.09 mg (67%)): mp 260 °C (dec); HRMS, for $C_{16}H_{14}N_5O_6$ (MH^+), calcd m/z 372.0944, obsd m/z 372.0945; ^{1}H NMR (DMSO-d_6) δ 2.65 (dd, 1H, J = 13.88, 8.30 Hz), 3.03 (dd, 1H, J = 13.88, 4.80 Hz), 4.26 (dd, 1H, J = 8.30, 4.80 Hz), 6.38 (s, 1H), 7.53 (s, 1H), 7.83 (s, 1H, exchangeable, NH), 7.99 (2H, d, J = 8.98 Hz), 8.31 (2H, d, J = 8.95 Hz), 10.60 (s, 1H, exchangeable, NH); ^{13}C NMR (DMSO-d_6) δ 31.5, 57.3, 102.8, 118.6, 122.1, 125.1, 129.6, 133.1, 146.7, 154.4, 157.4, 158.5, 164.3, 175.7.

Synthesis of 5-(3,4-Dihydroxybenzyl)hydantoin ($2_{red}H_2$). 5-(3,4-Dihydroxybenzyl)hydantoin ($2_{red}H_2$) was synthesized from 3,4-dibenzyloxybenzaldehyde in a manner similar to that for 5-(2,4,5-trihydroxybenzyl)hydantoin ($1_{red}H_3$): HRMS, for $C_{10}H_{11}N_2O_4$ (MH^+), calcd m/z 223.0719, obsd m/z 223.0723; ^{1}H NMR (DMSO-d_6) δ 2.73 (dd, 2H, J = 4.55, 8.00 Hz), 4.19 (t, 1H, J = 4.85 Hz), 6.42 (dd, 1H, J = 8.00, 1.95 Hz), 6.56 (d, 1H, J = 1.90 Hz), 6.60 (d, 1H, J = 8.0 Hz), 7.80 (s, 1H, exchangeable), 8.72 (br s, exchangeable), 10.35 (s, 1H, exchangeable); ^{13}C NMR (DMSO-d_6) δ 36.15, 58.94, 115.57, 117.57, 120.87, 126.52, 144.33, 145.04, 157.55, 175.68.

Methods. The ^{1}H NMR and ^{13}C NMR were performed on Bruker AM-400 MHz, AM-500 MHz, and AMX 400 spectrometers. All NMR samples in DMSO-d_6 were degassed using at least five freeze–pump–thaw cycles. Ultraviolet and visible absorbance data were obtained on an HP 8450A diode array spectrophotometer equipped with a thermostated cell holder at 25 ± 0.2 °C (path length 1 cm). Values of pH were determined on a doubly standardized Corning Ion Anal 260 pH meter. Mass spectra (MS) were obtained on a VG 70-SE or a VG ZAB 2-EQ instrument. TLC was performed on a silica gel sheet with a fluorescence indicator (EM Science). For column chromatography, silica gel 60, 0.063–0.200 mm (J.T. Baker), was used.

Acid–Base Titration. The acid–base dissociation constants were determined at 25 °C by spectrophotometric titration.

The pK_a of $1_{ox}H$: A 1-mL sample of the stock solution ($[1_{ox}^-]$ = 2.10 × 10^{-3} M) was diluted with 9 mL of a 0.1 M (μ = 0.3 with KCl) buffer of the desired pH, and UV–vis spectra were taken immediately after the dilution.

The pK_a of $1_{red}H_3$: A 3-mL buffer solution (0.1 M, μ = 0.3 with KCl) in a quartz cell with an 8-cm graded seal tube which was tightly closed with a septum rubber cap was degassed by bubbling Ar gas through it for 20 min. An excess amount of $NaBH_4$ (50 equiv) was added under an Ar stream, and then 50 μL of the stock solution ($[1_{red}H_3]$ = 8.93 ×

10^{-3} M, 0.1 N HCl) was injected into the solution. The spectra were taken immediately after the dilution.

The pK_a of BSAO: A 100-μL of sample of the enzyme stock solution in 0.1 M potassium phosphate buffer at pH 8.0 (SA, 0.33 u/mg; protein concentration, 17.5 mg/mL) was diluted with 400 μL of a HCl solution to give the desired pH. After the dilution, each enzyme sample was in 0.02 M buffer. The spectra were taken immediately after the dilution.

The pK_a of $7H_2$: A 3-mL buffer solution (0.05 M, $\mu = 0.5$ with KNO_3) in a quartz cell with an 8-cm graded seal tube which was tightly closed with a septum rubber cap was degassed by bubbling oxygen-free argon gas through it for 30 min. Oyxgen was removed from 99.999% argon gas by passing it through an alkaline pyrogallol solution. A 50-μL aliquot of the stock solution ($[7H_3^+] = 2.12 \times 10^{-2}$ M, 0.1 N degassed HCl) was injected into the buffer solution. The spectra were taken immediately after the dilution.

Electrochemistry. Cyclic voltammetry was carried out with a three-electrode system consisting of a glassy carbon working electrode (electrode area = 0.070 69 cm^2), a coiled platinum counter electrode, and a saturated calomel electrode. The voltammetric measurement was performed with a potentiostat (Princeton Applied Research 173) in conjunction with a triangular wave generator (Princeton Applied Research 175) and recorded on a X–Y recorder (Kipp and Zonen). Prior to each experimental run, the glassy carbon electrode was polished by alumina powder (Buehler alpha micropolish alumina, 1 mm), washed with alcohol and deionized water, and transferred rapidly to the electrochemical cell containing the test solution.

The experiment was carried out in Ar-purged solutions under at atmosphere of Ar at room temperature. The buffer solutions used and their pH, measured to ±0.01, were as follows: HNO_3 for pH 0–1.5, $CH_3COOH + HNO_3$ for pH 1–2, $CH_3COONa + HNO_3$ for pH 4–6.5, $NaH_2PO_4 + HNO_3$ for pH 6.5–8.5, tris(hydroxymethyl)aminomethane + HNO_3 for pH 8–9.5, $Na_2CO_3 + HNO_3$ for pH 9–11, $Na_3PO_4 + NaOH$ for pH 12–13, and NaOH for pH > 12.5. The ionic strength of the buffer solution was adjusted to 0.5 with KNO_3. Stock solutions of $\mathbf{1}_{red}H_3$ and $\mathbf{2}_{red}H_2$ were prepared in 0.01 N HCl at a concentration of 1.0×10^{-2} M, respectively. The test solution was prepared with 0.4 mL of stock solution being added to 9.6 mL of the buffer prior to the run. For the aminophenol ($7H_2$), the stock solution was prepared in 0.1 N HCl at a concentration of 4×10^{-3} M, and the test solution was prepared with 1 mL of the stock solution being added to 9 mL of a buffer.

NMR Assignment of the 4-Nitrophenylhydrazone Derivative of Topa Quinone Hydantoin Quinone (3). ^1H and ^{13}C NMR spectra of **3** were obtained on a Bruker AMX 400 spectrometer fitted with a QNP probe, operating at a proton frequency of 400.13 MHz except for the long-range inverse proton carbon correlation (HMBC), which was acquired on a Bruker AM-500 fitted with an inverse ^1H–^{13}C probe operating at 500.13 MHz for protons. A 0.3 M solution was used for the 2D experiments. All spectra were recorded at 22 °C. ^1H NMR chemical shifts are relative to a residual DMSO-d_5 signal set to 2.490 ppm. ^{13}C chemical shifts are relative to the ^{13}C signal of DMSO-d_6 set to 39.50 ppm. The ROESY spectrum was acquired using the method of Kessler et al.,[8] which uses a small-angle hard pulse train to generate a spin lock. The mixing time was 200 ms; 512 t_1 increments of 1 K data points were recorded, using a pure absorption mode (TPPI). The ^1H–^{13}C HMQC experiment used the standard pulse sequence[9] in the absorption mode; 512 t_1 increments of 2 K data points were collected. The long-range inverse ^1H–^{13}C correlation[10] was processed in magnitude mode; 512 t_1 increments of 2 K data points were collected. A delay of 60 ms was used in the pulse sequence to allow for evolution of long-range couplings. All 2D spectra were zero fitted to twice their original size in both dimensions prior to processing.

Results and Discussion

Synthesis and Characterization of Model Compounds. The reduced form of the topa quinone hydantoin ($\mathbf{1}_{red}H_3$, eq 2) was isolated in 87% yield by use of acidic ethanol as a solvent in the deprotection of the benzyloxy groups of 5-(2,4,5-tribenzyloxybenzyl)hydantoin. The quinol was only stable in an acidic solution and was air-oxidized to the quinone in the presence of a catalytic

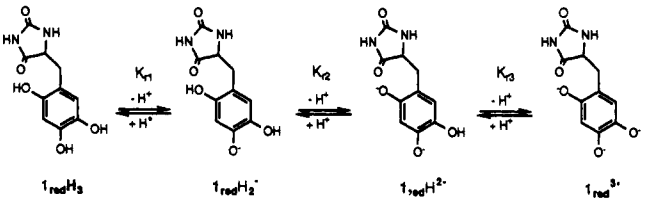

(2)

amount of triethylamine in dry methanol. The quinone was isolated as a very unstable solid both in the protonated form ($\mathbf{1}_{ox}H$, eq 3) and in the salt form ($\mathbf{1}_{ox}^-Na^+$) after silica gel chromatography. Treatment of $\mathbf{1}_{ox}^-Na^+$ with an acid easily

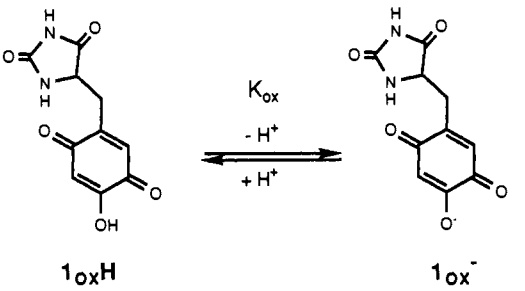

(3)

generated $\mathbf{1}_{ox}H$. When $NaIO_4$ was used as a catalyst to generate quinone from quinol, a purple compound, in which one of the ring protons is missing, was obtained as a major product (cf. Experimental Procedures).

The ^1H NMR spectrum of $\mathbf{1}_{red}H_3$ in DMSO-d_6 shows a pair of doublets at δ 2.46 and 2.90 which are assigned to the CH_2 group of the hydantoin. This splitting is attributed to hindered rotation and/or the existence of an intramolecular hydrogen bonding between a carbonyl of the hydantoin and the C2 OH on the phenyl ring, since no splitting is observed for the (dihydroxybenzyl)hydantoin ($\mathbf{2}_{red}H_2$). A similar splitting is also seen in the quinone ($\mathbf{1}_{ox}H$ and $\mathbf{1}_{ox}^-Na^+$). In this case, an NH of the hydantoin and the carbonyl C2 quinone are capable of hydrogen bonding. The protons at 6.07 ppm in $\mathbf{1}_{ox}H$ and at 5.00 ppm in $\mathbf{1}_{ox}^-$ are assigned to the ring protons involved in an acid-catalyzed enol tautomerization,[3] as evidenced by loss of these signals in DCl.

6-Amino-4-ethylresorcinol ($7H_2$) was synthesized as a model compound of the aminophenol, which has been proposed as a reaction intermediate in amine oxidation by BSAO.[6,11] $7H_2$ was made by the reduction of 4-ethyl-6-nitrosoresorcinol (**6**) with $SnCl_2$ in concentrated HCl. It should be noted that this nitrosoresorcinol (**6**) is in equilibrium with its hydroxybenzoquinone monooxime tautomer (**8**) on the basis of the ^1H NMR

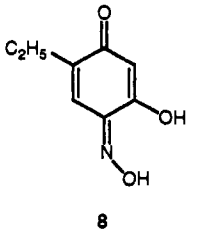

8

chemical shifts (cf. Experimental Procedures), and it is easily hydrolyzed directly to the corresponding hydroxybenzoquinone (**10**, in Scheme I) under acidic conditions.[12] Thus, preparation of **6** requires its immediate separation from its acidic reaction mixture. We note that $7H_2$ could not be isolated from reaction mixtures involving reduction of **6** with alkaline hydrosulfite, $NaBH_4$, or catalytic hydrogenation. This is attributed to a

(8) Kessler, H.; Griesinger, C.; Kerssebaum, R.; Wagner, K.; Ernst, R. R. *J. Am. Chem. Soc.* **1987**, *109*, 607–609.
(9) Bax, A.; Subramanian, S. *J. Magn. Reson.* **1985**, *67*, 565–569.
(10) Bax, A.; Summers, M. F. *J. Am. Chem. Soc.* **1986**, *108*, 2093–2094.
(11) Hartmann, C.; Klinman, J. P. *Biochemistry* **1991**, *30*, 4605–4611.
(12) Cf. McLamore, W. M. *J. Am. Chem. Soc.* **1951**, *73*, 2225–2230.

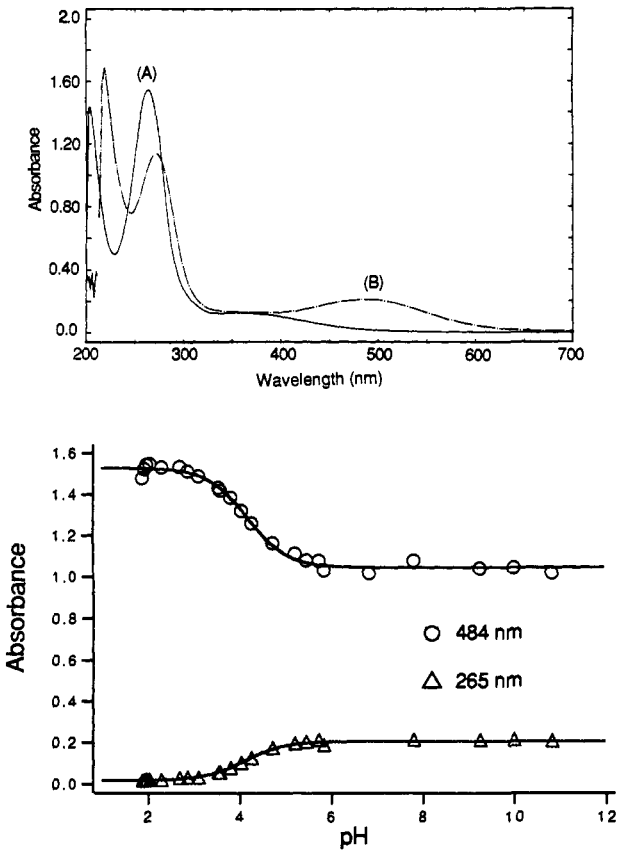

Figure 1. (top) Absorption spectra of (A) $\mathbf{1}_{ox}H$ at pH 2.04 and (B) $\mathbf{1}_{ox}^-$ at pH 5.72. (bottom) Spectroscopic pK_a determinations for $\mathbf{1}_{ox}H$. Lines were drawn by least squares fits using the following equations: $A_{265} = (\epsilon_{265}^{\mathbf{1}_{ox}H}\{[H^+]/\{K_{ox} + [H^+]\}\} + \epsilon_{265}^{\mathbf{1}_{ox}^-}\{K_{ox}/\{K_{ox} + [H^+]\}\})[\mathbf{1}_{ox}H]_T$ and $A_{484} = (\epsilon_{484}^{\mathbf{1}_{ox}H}\{[H^+]/\{K_{ox} + [H^+]\}\} + \epsilon_{484}^{\mathbf{1}_{ox}^-}\{K_{ox}/\{K_{ox} + [H^+]\}\})[\mathbf{1}_{ox}H]_T$.

Scheme I. Oxidation of the Aminophenol ($7H_2$) to the Iminoquinone (**9**) at pH 9.0, Alkaline Hydrolysis to the Quinone (**10**), and Transamination with Benzylamine to the Substrate Schiff Base (**11**)

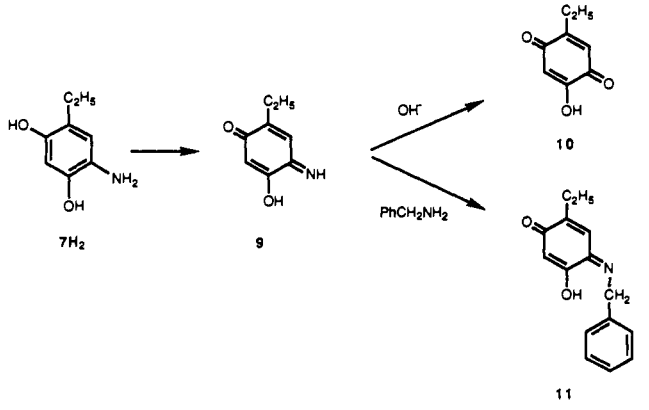

conversion of $7H_2$ to dye-like compounds such as indophenol and resorufin[13] in the workup steps.

Aqueous Acid–Base Chemistry. The acid–base dissociation constant (pK_{ox} in eq 3) for $\mathbf{1}_{ox}H$ was measured at 25 °C by spectrophotometric titration. The color of the quinone solution changed from pale yellow to red with increasing pH. This was found to be due to the appearance of an absorbance at 484 nm and a decrease in absorbance at 265 nm with isosbestic points at 243 and 277 nm (Figure 1 (top)). Plots of A_{265} and A_{484} *vs* pH fit the titration curves for the dissociation of a single proton, allowing the calculation of a pK_a of 4.13 ± 0.01 by least-squares analysis (Figure 1 (bottom)).

(13) Musso, H. *Angew. Chem.* **1961**, *73*, 665.

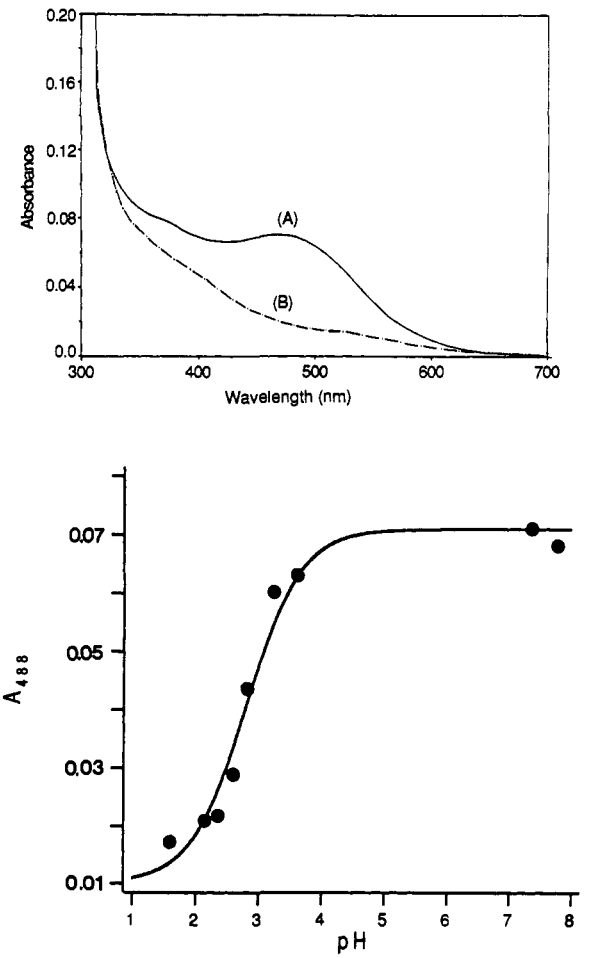

Figure 2. (top) Absorption spectra of BSAO (A) at pH 7.77 and (B) at pH 1.59. (bottom) Spectroscopic pK_a determination for BSAO. The line was drawn by a least-squares fit using the following equation: $A_{488} = (\epsilon_{488}^{\text{acid form}}\{[H^+]/\{K_a + [H^+]\}\} + \epsilon_{488}^{\text{base form}}\{K_a/\{K_a + [H^+]\}\})[\text{BSAO}]_T$.

The pK_a of the oxidized form of the enzyme (BSAO) was determined at 25 °C by spectrophotometric titration. The spectrum of the native enzyme (BSAO) has a characteristic absorption around 484 nm at neutral pH [(A) in Figure 2 (top)]. This absorption disappeared upon addition of acid [(B) in Figure 2 (top)]. This spectral change was reversible for a short time, although the enzyme was gradually denatured in an acidic solution. Plots of A_{484} *vs* pH fit the titration curve for the dissociation of a single proton, giving a pK_a of 3.0 ± 0.2 by least-squares analysis (Figure 2 (bottom)). This value is ca. 1.0 pH unit lower than that of the model compound ($\mathbf{1}_{ox}H$). In other words, the anionic form of the cofactor ($\mathbf{1}_{ox}^-$) is more stable in the enzyme active site pocket than a nonbound form in an aqueous solution. This result may be explained as follows: (i) The active site copper (Cu^{2+}) adjacent to the C2 carbonyl group may contribute to the stabilization of the anionic form; distance mapping experiments support the placement of Cu^{2+} near this position of the cofactor.[14] (ii) A positively charged amino acid side chain could reside in the active site, leading to electrostatic stabilization of the ionized form of the cofactor.

The pK_a values for $\mathbf{1}_{red}H_3$ (pK_{r1}, pK_{r2}, and pK_{r3} in eq 2) were determined spectrophotometrically in the presence of $NaBH_4$ as an antioxidant under anaerobic conditions. An increase of pH from 7.8 to 13.2 resulted in an observed shift of λ_{max} from 295 to 315 nm (Figure 3 (top)). pK_{r1} and pK_{r2} were calculated to be 9.17 ± 0.17 and 11.66 ± 0.03, respectively, by least-squares

(14) (a) Williams, T. J.; Falk, M. C. *J. Biol. Chem.* **1986**, *261*, 15949–15954. (b) Dooley, D. M.; McGuirl, M. A.; Cote, C. E.; Knowles, P. F.; Singh, I.; Spiller, M.; Brown III, R. D.; Koenig, S. H. *J. Am. Chem. Soc.* **1991**, *113*, 154–761.

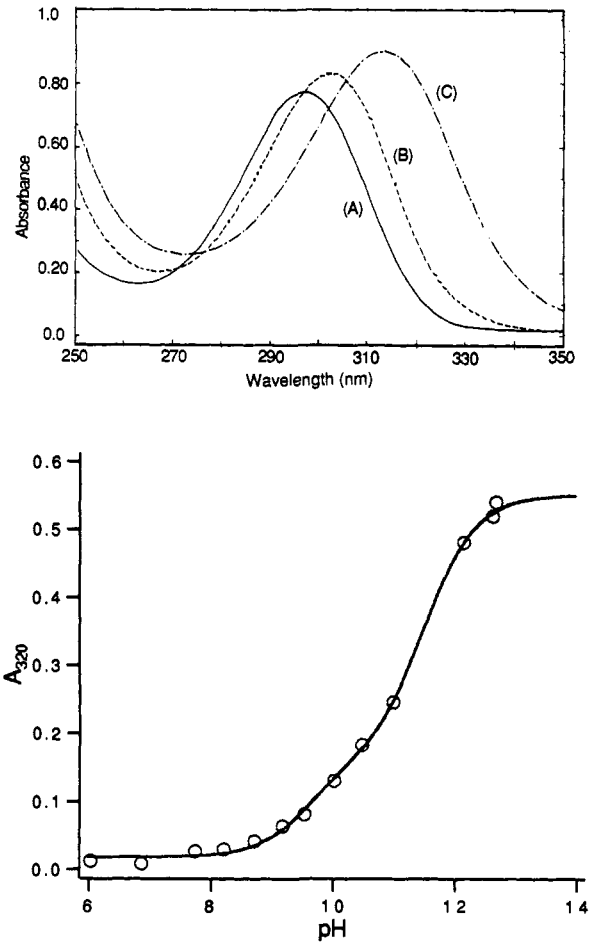

Figure 3. (top) Absorption spectra of (A) $\mathbf{1}_{red}H_3$ at pH 7.5, (B) $\mathbf{1}_{red}H_2^-$ at pH 11.0, and (C) $\mathbf{1}_{red}H^{2-}$ at pH 12.9. $[\mathbf{1}_{red}H_3] = 1.97 \times 10^{-4}$ M. (bottom) Spectroscopic pK_a determination for $\mathbf{1}_{red}H_3$. $[\mathbf{1}_{red}H_3] = 1.44 \times 10^{-4}$ M. The line was drawn by a least-squares fit using the following equation: $A_{320} = (\{\epsilon_{320}^{\mathbf{1}_{red}H_3}[H^+]^2 + \epsilon_{320}^{\mathbf{1}_{red}H_2^-}K_{r1}[H^+] + \epsilon_{320}^{\mathbf{1}_{red}H^{2-}}K_{r1}K_{r2}\}/\{[H^+]^2 + K_{r1}[H^+] + K_{r1}K_{r2}\})[\mathbf{1}_{red}H_3]_T$.

analysis of the absorbance change at 320 nm (Figure 3 (bottom)). pK_{r3} was estimated to be greater than 12.2 from the absorbance change at 350 nm. However, above pH 13, new absorption maxima appeared at 416 and 436 nm with a shoulder at 350 nm (data not shown), precluding an accurate determination of pK_{r3}. This high pH spectrum was observed to be very similar to that of the semi-quinone radical of 2-hydroxy-1,4-benzoquinone, obtained by radiolytic oxidation of 1,2,4-benzenetriol.[15] There is a ca. 5 pH unit difference between the pK_a value of the hydroxyl group in the oxidized form ($\mathbf{1}_{ox}H$) *vs* the reduced form ($\mathbf{1}_{red}H_3$) of topa hydantoin. In the case of $\mathbf{1}_{ox}H$, the resonance effect involving delocalization of electrons is expected to stabilize the anionic structure ($\mathbf{1}_{ox}^-$) and lower the pK_a value.

The pK_a values for the aminophenol ($7H_3^+$) (shown in eq 4) were determined spectrophotometrically under oxygen-free conditions. At pH 4, the aminophenol ($7H_3^+$) has a λ_{max} at 274 nm;

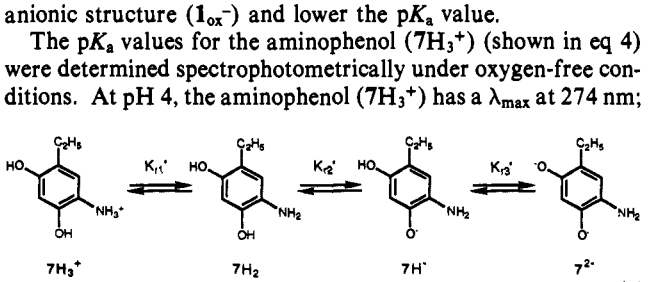

(4)

with increasing pH, this shifts to give a new absorption maxima at 322 nm, which is 7 nm red-shifted compared to the quinol

(15) Qin, L.; Tripathi, G. N. R.; Schuler, R. H. *J. Phys. Chem.* **1987**, *91*, 1905–1910.

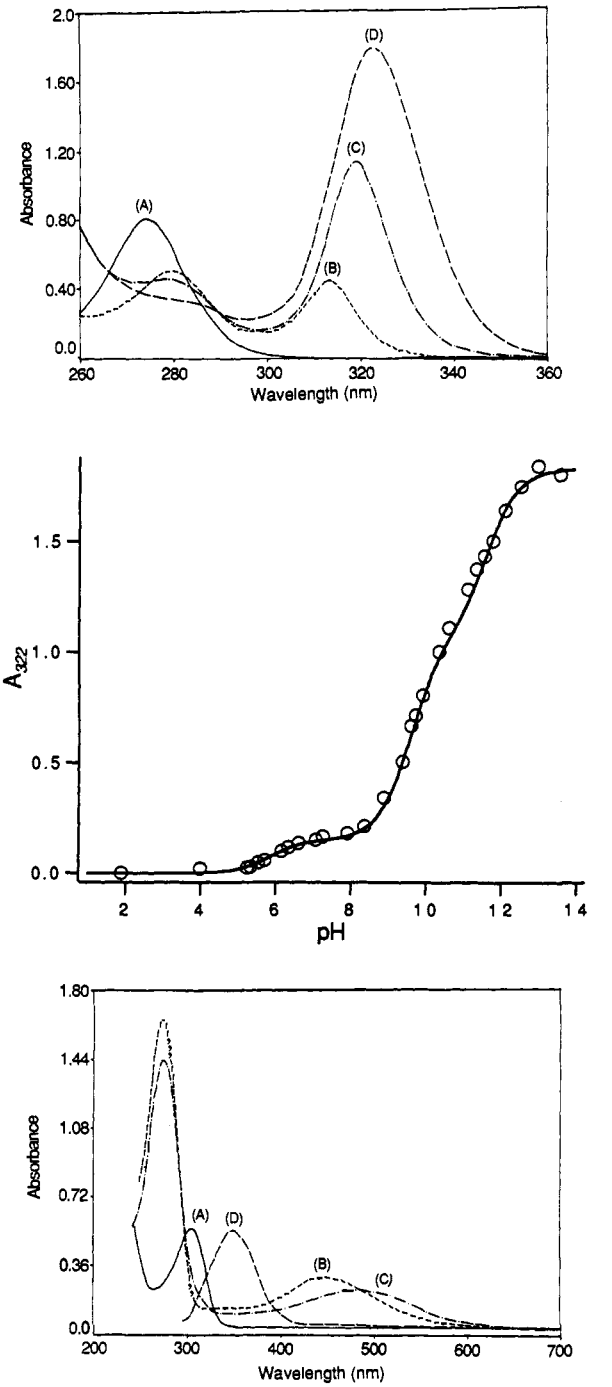

Figure 4. (top) Absorption spectra of (A) $7H_3^+$ at pH 3.9, (B) $7H_2$ at pH 7.1, (C) $7H^-$ at pH 10.4, and (D) 7^{2-} at pH 13.6. (middle) Spectroscopic pK_a determination for $7H_3^+$. $[7H_3^+] = 3.48 \times 10^{-4}$ M. The line was drawn by a least-squares fit using the following equation: $A_{322} = (\{\epsilon_{322}^{7H_3^+}[H^+]^3 + \epsilon_{322}^{7H_2}K_{r1}'[H^+]^2 + \epsilon_{322}^{7H^-}K_{r1}'K_{r2}'[H^+] + \epsilon_{322}^{7^{2-}}K_{r1}'K_{r2}'K_{r3}'\}/\{[H^+]^3 + K_{r1}'[H^+]^2 + K_{r1}'K_{r2}'[H^+] + K_{r1}'K_{r2}'K_{r3}'\})[7H_2]_T$. (bottom) Absorption spectra of (A) $7H_2$ at pH 9.0, (B) aeration of (A), (C) (B) after 1 h, and (D) addition of benzylamine to (B). $[7H_2] = 1.31 \times 10^{-4}$ M.

(Figure 4 (top)). Three pK_a's were calculated to be 5.88, 9.59, and 11.62, respectively, by least-squares analysis of the absorption change at 322 nm (Figure 4 (middle)). The lowest pK_a seems to be that of the amino group on the basis of the pK_a value of aniline.[16] The aminophenol and the quinol have no 484-nm absorption band, comparable to the reduced form of copper amine oxidases generated by substrate amine[17,18] and $Na_2S_2O_4$,[19]

(16) *Handbook of Biochemistry and Molecular Biology*; Fasman, G. D., Ed.; CRC Press: Cleveland, OH, 44128.

(17) Petterson, G.; Lindstrom, A. *Eur. J. Biochem.* **1978**, *83*, 131–135.

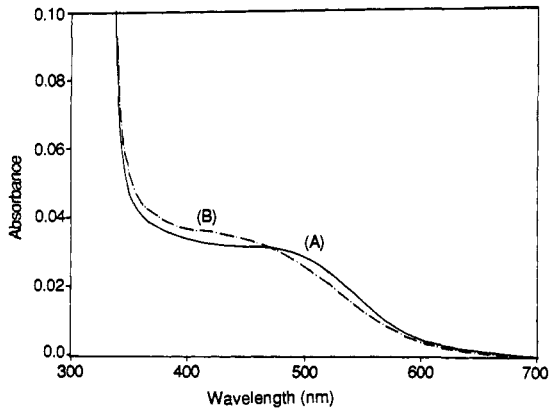

Figure 5. Absorption spectra of (A) BSAO in carbonate buffer, pH 9.17, and (B) the BSAO–ammonia complex; [BSAO] = 1.75 mg/mL, [NH_3] = 6.99×10^{-3} M (which is calculated using pK_a = 9.24 of NH_4^+),[16] pH 9.13.

respectively, under anaerobic conditions. At pH 9.0, the aminophenol ($7H_2 + 7H^-$) was rapidly air-oxidized to a compound with λ_{max} at 274 and 448 nm [(B) in Figure 4 (bottom)], which is a ca. 40-nm blue shift compared with that of the quinone [(B) in Figure 1 (top)]. It is interesting to note that a similar 40-nm blue shift was also observed in the case of the ammonia complex of BSAO (Figure 5). The absorption spectrum with λ_{max} at 448 nm was gradually converted to the deprotonated form of the corresponding hydroxyquinone (**10** in Scheme I) with characteristic λ_{max} at 484 nm [(C) in Figure 4 (bottom)]. When it was treated with a large excess of benzylamine, a spectrum with λ_{max} at 350 nm was immediately observed [(D) in Figure 4 (bottom)]. Although this spectrum is closely similar to that of the first intermediate formed upon addition of benzylamine to BSAO,[20] it is attributed to the product imine formed by a transamination reaction (see below). These observations indicate that the aminophenol ($7H_2 + 7H^-$) is easily oxidized to the iminoquinone (**9**, Scheme I). Alkaline hydrolysis generates the quinone (**10**, Scheme I). Addition of benzylamine produces the imine by a transimination reaction (**11**, Scheme I). The origin of different λ_{max} values for **9** (448 nm) *vs* **11** (350 nm) is attributed to further reaction of **11** to yield the product imine, which is characterized by a ca. 10-fold greater extinction coefficient at this wavelength than that for the substrate imine.[35] The iminoquinone (**9**) seems to be more reactive than the quinone (**10**), since reaction of **10** with benzylamine was appreciably slower at this pH. The pK_a of the iminoquinone (**9**) was not determined since the quinone monoimine is known to undergo deamination (hydrolysis) catalyzed either by an acid or by a base.[21]

Electrochemistry. Electrochemical redox potentials of topa hydantoin quinone ($\mathbf{1}_{ox}H$) and dopa hydantoin quinone ($\mathbf{2}_{ox}$), were compared as a function of pH, by employing cyclic voltammetry with a glassy carbon electrode (*vs* SCE). Figure 6 (top) shows the pH-dependence of the cyclic voltammograms for $\mathbf{1}_{ox}H$ and reveals a single process for the oxidation and reduction between pH 1.1 and 13.1. No decomposition was observed during the cyclic voltammogram scan. At pH 2, the peak separation of the anodic and cathodic peaks (ΔE_p) is 30 mV, which is in agreement with the theoretical one for a reversible one-step two-electron mechanism. Then the ΔE_p increased with pH to give a quasi-reversible cyclic voltammogram. The redox potentials of quinone/semiquinone and semiquinone/quinol couples could not been determined from the quasi-reversible cyclic voltammograms.

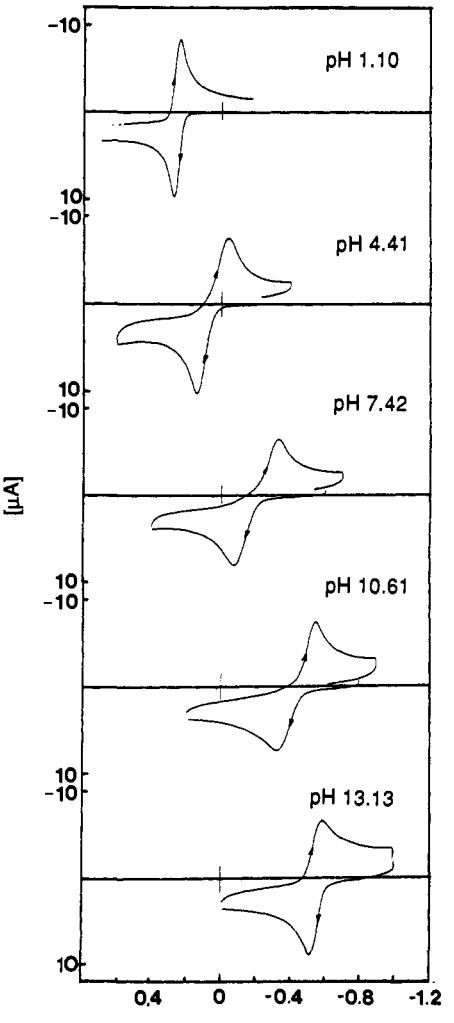

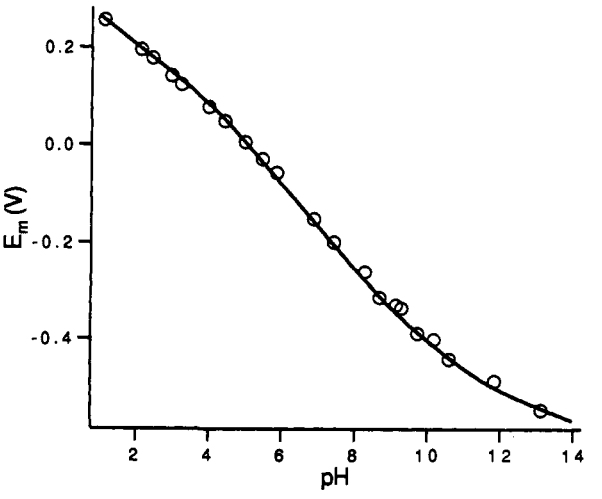

Figure 6. (top) pH-dependence of cyclic voltammograms for **1** (4.0×10^{-4} M) at a scan speed of 100 mV s^{-1}. The direction of the scan is from negative to positive. (bottom) E_m–pH diagram for **1**. The line was drawn by a least-squares fit using the following equation: $E_m = E_0 + (RT/nF) \log(\{[H^+]^3 + K_{r1}[H^+]^2 + K_{r1}K_{r2}[H^+] + K_{r1}K_{r2}K_{r3}\}/\{[H^+] + K_{ox}\})$ (E_0 is the half-wave potential at pH 0).

Figure 6 (bottom) is a plot showing the pH dependence of the midpoint potentials of overall $2e^-$ transfer for $\mathbf{1}_{ox}H$. The solid line was generated using values of pK_{ox} from Figure 1 (bottom) and pK_r from Figure 3 (bottom). The third pK_a of $\mathbf{1}_{red}H_3$ (pK_{r3}) was calculated as 13.0 from the least-squares curve fitting.

(18) Palcic, M. M.; Klinman, J. P. *Biochemistry* **1983**, *22*, 5957–5966.
(19) Yamada, H.; Yasunobu, K. T. *J. Biol. Chem.* **1962**, *237*, 1511.
(20) Hartmann, C.; Brzovic, P.; Klinman, J. P. *Biochemistry* **1993**, *32*, 2234–2241.
(21) Brown, E. R. In *The Chemistry of Quinonoid Compounds*, Vol. II; Patai, S., Rappoport, Z., Eds.; John Wiley and Sons: New York, NY, 1988; Chapter 21.

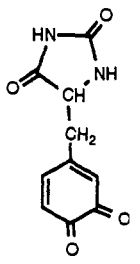

2_{ox}

The E_m *vs* pH plot (Figure 6 (bottom)) is composed of five linear lines with slopes -59.9 mV/pH (pH 1–4), -88.0 mV/pH (pH 4.5–8.5), -60 mV/pH (pH 10–11), -31 mV/pH (pH 12–12.5), and 0 mV/pH (pH > 13). Below pH 4, $\mathbf{1}_{red}H_3$ is oxidized to the quinone ($\mathbf{1}_{ox}H$) in the usual $2H^+, 2e^-$ process (eq 5). Between

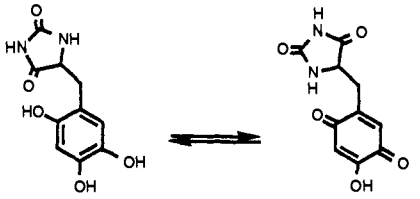

$+ 2e^- + 2H^+$ (5)

pH 4.5 and 8.5, the slope of -90 mV/pH corresponds to a $3H^+$, $2e^-$ redox process due to the acid dissociation of the hydroxyl group in the resulting quinone. Between pH 10 and 11, one of the hydroxyl groups of the reduced quinol is deprotonated (pK_{r1} = 9.17), so that once again it is oxidized in a $2H^+$, $2e^-$ process. Between pH 12 and 12.5, the second acid dissociation of the reduced quinol (pK_{r2} = 11.66) results in the slope of -30 mV/pH, which corresponds to a $1H^+$, $2e^-$ process. Finally, above pH 13, the reduced form is in a fully deprotonated form (pK_{r3} = 13.0), yielding a slope of 0 mV/pH.

The cyclic voltammetry of dopa quinone hydantoin quinone ($\mathbf{2}_{ox}$) was studied between pH 1.1 and 13.2. The E_m values are plotted in Figure 7 (top) as a function of pH. Below pH 8.5, this plot has a -60 mV/pH slope, confirming that the electrode reaction observed is the expected two-electron and two-proton process (eq 6).

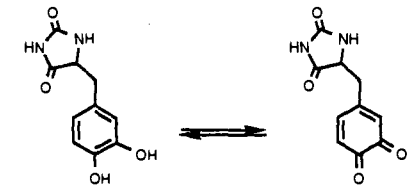

$+ 2e^- + 2H^+$ (6)

The electrochemistry of dopa (3,4-dihydroxyphenylalanine) has been studied extensively.[22] It is well-known that dopa is oxidized to dopaquinone; above pH 4, the dopaquinone is converted to side chain cyclized products[5] such as leucodopachrome. In our hands, the dopa hydantoin quinone ($\mathbf{2}_{ox}$) was stable at pH below 8.5. For solutions above pH 9, the CV became asymmetric and a new redox couple in agreement with that of topa quinone hydantoin ($\mathbf{1}_{ox}^-$) appeared. The formation of topa quinone hydantoin was also confirmed by the color change of the solution from yellow to pink (λ_{max} at 484 nm). Figure 7 (bottom) shows the CV at pH 13.2. The CV for the oxidation was completely irreversible with no suggestion of any reduction. The redox couple at E_m = -537.5 mV corresponds to that of $\mathbf{1}_{ox}^-$ (E_m = -539.2 mV). This indicates that dopa hydantoin quinone undergoes an

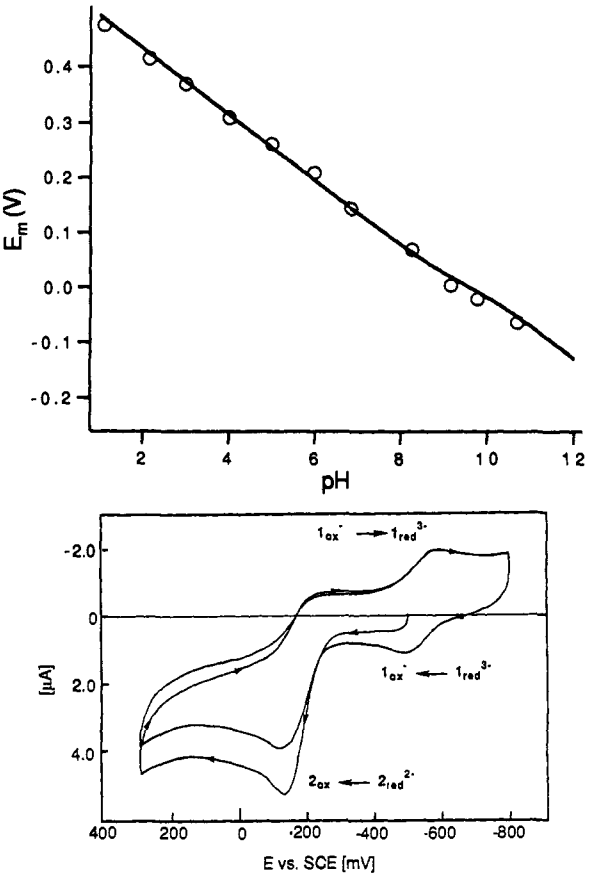

Figure 7. (top) E_m–pH diagram for **2**. The line was drawn by a least-squares fit using the following equation: $E_m = E_0 + (RT/nF)\log(\{[H^+]^3 + K_{r1}[H^+]^2\}/\{[H^+] + K_{ox}\})$ (E_0 is the half-wave potential at pH 0). (bottom) Cyclic voltammograms of **2** at pH 13.0, 100 mV s^{-1}.

Scheme II. Generation of the Topa Quinone ($\mathbf{1}_{ox}^-$) from the Dopa Quinone ($\mathbf{2}_{ox}$) at Alkaline pH

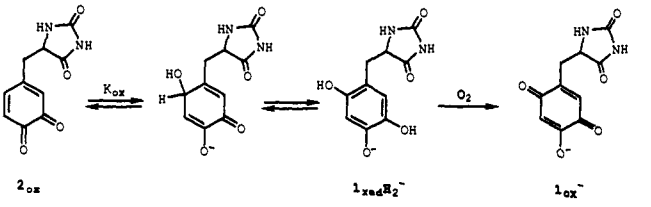

acid–base equilibrium with its pseudobase above pH 9 as shown in Scheme II. The pK_a values for the pseudobase formation (K_{ox}, Scheme II) and the first ionization of $\mathbf{2}_{red}H_2$ were estimated as 10.0 and 8.99 by least-squares curve fitting of the data in Figure 7 (top).

We have demonstrated that topa is derived from an active site tyrosine.[5] As described, the oxidation of tyrosine to dopa may be catalyzed by a tyrosinase-like enzyme or the active site metal ion (Cu^{2+}).[5] The present observation indicates that the conversion of dopa to topa could proceed nonenzymatically through a 1,4-addition of water to dopa quinone. It should be noted that the extra hydroxyl group in topa relative to dopa decreases the redox potential by ca. 300 mV and, further, that topa and PQQ[23] have an equal thermodynamic capacity to carry out a $2e^-$ oxidation in an aqueous solution at pH 7.2.

The cyclic voltammetry of the iminoquinone (**9**, Scheme I) was measured at pH 6.8 and 9.6. The iminoquinone (**9**) was found to be stable during the initial CV scan from UV spectroscopy. However, the coupling reaction with the aminophenol ($\mathbf{7}H_2$) to form a purple indophenol-type dye was observed

(22) (a) Hawley, M. D.; Tatawawadi, S. V.; Piekarski, S.; Adams, R. N. *J. Am. Chem. Soc.* **1987**, *89*, 447–450. (b) Brun, A.; Rosset, R. *J. Electroanal. Chem. Interfacial. Electrochem.* **1974**, *49*, 287–300. (c) Young, T. E.; Babbit, B. W.; Wolfe, L. A. *J. Org. Chem.* **1980**, *45*, 2899–2902.

(23) Kano, K.; Mori, K.; Uno, B.; Kubota, T.; Ikeda, T.; Senda, M. *Bioelectrochem. Bioenerg.* **1990**, *23*, 227–238.

Table I. Midpoint Potentials for $\mathbf{1}_{ox}$ and 9[a]

	pH	E_m, mV (vs SCE)
1	6.78	−150
	9.56	−380
9	6.78	−133
	9.56	−365

[a] As described in the Experimental Procedures, cyclic voltammetry was performed on the reduced species $\mathbf{1}_{red}$ and 7. The formation of $\mathbf{1}_{ox}$ and 9 is transient and occurs at the electrode surface.

after repetitive scans. The E_m values of 9 at pH 6.8 and 9.6 are shown in Table I together with those of the quinone ($\mathbf{1}_{ox}^-$). It can be seen that the redox potential of the iminoquinone (9) is slightly more positive (ca. 17 mV) than that of the quinone ($\mathbf{1}_{ox}^-$), both at pH 6.78 and 9.56.

Synthesis and Characterization of the (4-Nitrophenyl)hydrazone Derivative (3). We have demonstrated that topa quinone is the organic cofactor in a number of copper amine oxidases.[3,4] The identification of the cofactor has been achieved by derivatization of the cofactor with phenylhydrazine or (4-nitrophenyl)hydrazine to form a stable hydrazone adduct, followed by spectroscopic characterization of either intact proteins[4] or active site derived peptides.[3,4,5] The position of the nucleophilic addition has been estimated to be at C5, the carbonyl carbon next to the hydroxyl group.[3] Here, we used 2D NMR experiments to assign the structure in the (4-nitrophenyl)hydrazone derivative of topa quinone hydantoin, isolated from the reaction of topa quinone hydantoin and an excess amount of (4-nitrophenyl)hydazine hydrochloride.

The ^{13}C chemical shifts of the (4-nitrophenyl)hydrazone derivative in DMSO-d_6 indicate that the azo tautomeric form is predominant, since the chemical shifts for quinonoid carbonyl carbons would be at significantly higher frequencies than those observed (ca. 180 ppm) (cf. Experimental Procedures). Hydrazones are well-known to undergo hydrazone–azo tautomerism, and the equilibrium between the forms is strongly influenced by the nature of the molecule, solvent, or temperature.[24] The slow D exchange of the ring proton at C3 suggests that the hydrazone exists as a minor component in equilibrium with the azo structure (Scheme III). In addition to 3, two other structures for the (4-nitrophenyl)hydrazone are possible:

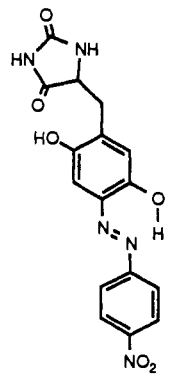

4

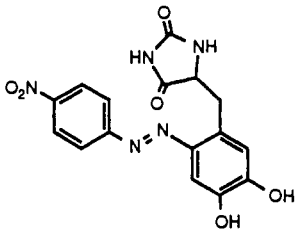

5

Discrimination among the three structural isomers was achieved by detailed NMR studies, documented below.

The ^1H NMR spectrum shows the same pattern of splitting for the CH_2 protons of the hydantoin methylene group as observed with topa hydantoin quinol and quinone. The doublets at 7.99 and 8.31 ppm are assigned as the ring protons of the (nitrophenyl)hydrazone from the similarity of their coupling constants. The singlets at 7.83 and 10.60 ppm are rapidly exchangeable

(24) Krueger, P. J. In *The Chemistry of the Hydrazo, Azo, and Azoxy Groups*; Patai, S., Ed.; John Wiley and Sons: New York, NY, 1975; pp 151–224.

Scheme III. Hydrazo–Azo Tautomeric Structures of the (4-Nitrophenyl)hydrazine Adduct of the Topa Quinone (3) (the Slow Deuterium Exchange of the Ring Proton at C3 Suggests that the Hydrazone Exists as a Minor Component in the Equilibrium)

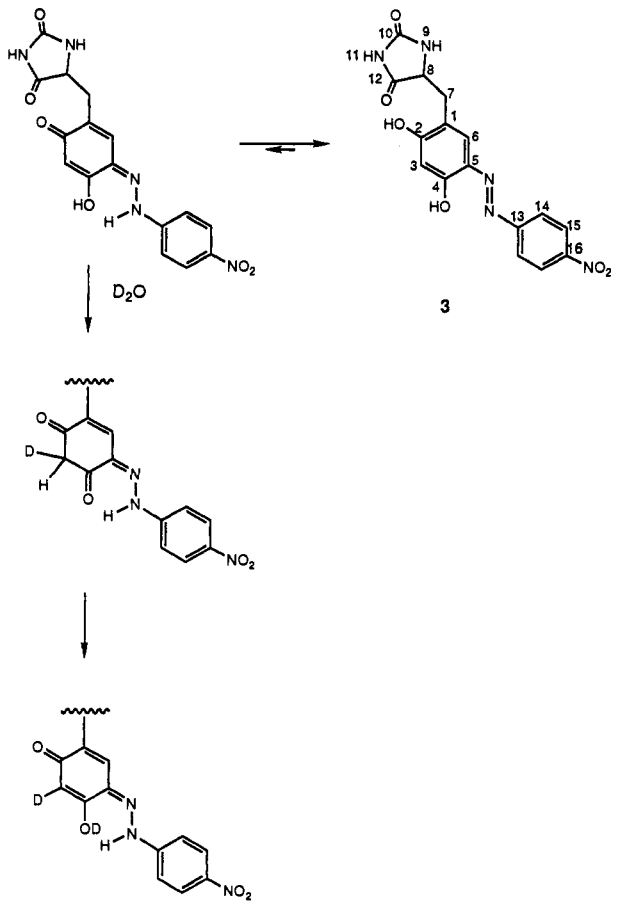

with D (D_2O) and are assigned as NH protons of the hydantoin group on the basis of chemical shifts. These protons also show clear NOE cross peaks to the protons attached to the methylene (H7a, H7b) and methine (H8) of the hydantoin (data not shown). As noted above, the ring proton at C3 (6.38 ppm) is exchangeable with D (D_2O) although the reaction is very slow. HMQC experiments established the connectivities of protons directly bound to carbon. The connectivities between H3 and C3, H6 and C6, H7a, H7b and C7, H8 and C8, H14 and C14, and H15 and C15 were observed. The substitution pattern of the central tetra-substituted benzene ring was derived from the fact that in a HMBC experiment (Table II), the protons attached to C7 (H7a and H7b) show correlations to C2, C6, and C12, and the proton attached to C6 (H6) shows correlation to C2, C4, and C7, all via $^3J_{H-C}$. The ^{13}C chemical shifts at 133.1 and 158.5 ppm are assigned to be C5 and C4, respectively, as follows: (i) A $^3J_{C-H}$ (three-bond coupling) is larger than $^2J_{C-H}$ (two-bond coupling) in a benzene ring.[25] The intensity of the cross peaks between H3 and a carbon at 133.1 ppm is larger than that between H3 and a carbon at 158.5 ppm. On the other hand, H6 exhibits a more intense response with a carbon at 158.5 ppm than with a carbon at 133.1 ppm (Table II). It, therefore, is assumed that the carbon at 133.1 ppm is C5 and the carbon at 158.5 ppm is C4. (ii) An aromatic carbon which is attached to an OH group has a chemical shift at around 157 ppm (cf. Experimental Procedures; $\mathbf{1}_{ox}^-$, $\mathbf{2}_{red}H_2$). (iii) The calculated ^{13}C shifts for the structure 3 shown in Table III are in good agreement with the observed values. In

(25) Hansen, P. E. *Prog. Nucl. Magn. Reson. Spectrosc.* **1981**, *14*, 175.
(26) *Tables of Spectral Data for Structure Determination of Organic Compounds*; Pretsch, E., Clerc, T., Seibl, J., Simon, W., Eds.; Springer-Verlag: New York, NY, 1989.

Table II. ^1H and ^{13}C NMR Data for **3** in DMSO-d_6

position number[a]	δH	H coupled with H	δC	H coupled with C
1			118.6	H3 (m),[b] H7a (m), H7b (m), H8 (s)
2			164.3	H6 (w), H7a (w), H7b (w)
3	6.38		102.8	
4			158.5	H3 (m), H6 (s)
5			133.1	H3 (s), H6 (m)
6	7.53		129.6	H7a (m), H7b (m)
7a	2.65	H7b, H8	31.5	H6 (m), H8 (w)
7b	3.03	H7a, H8		
8	4.26	H7a, H7b	57.3	H7a (s), H7b (s), H9 (m), H11 (s)
9	7.83			
10			157.4	H8 (m), H9 (m), H11 (s)
11	10.60			
12			175.7	H7a (s), H7b (s), H8 (s), H9 (s), H11 (w)
13			154.4	H15 (m)
14	7.99	H15	122.1	
15	8.31	H14	125.1	
16			146.7	H14 (cm), H15 (m)

[a] For the numbering system, see structure **3** in Scheme III. [b] Relative intensity of the cross peak.

Table III. Comparison of Computed and Observed C13 Chemical Shifts for the Three 4-Nitrophenylhydrazone Topa Quinone Hydantoin Isomers **3**, **4**, and **5**

carbon number[a]	calculated chemical shifts[b]			observed chemical shifts[c]
	3	**4**	**5**	
1	124.5	135.1	132.5	118.6
2	158.4	147.8	146.0	164.3
3	103.3	111.3	111.3	102.8
4	148.2	138.4	140.2	158.5
5	132.4	142.2	144.8	133.1
6	124.9	116.9	116.9	129.6
13	158.5			154.4
14	123.5			122.1
15	123.5			125.1
16	150.3			146.7

[a] For the numbering system, see structure **3** in Scheme III. [b] Relative to TMS. Calculation was done by use of empirical data.[26] [c] Relative to the residual DMSO-d_6 signal set to 39.50 ppm.

a ROESY experiment (Figure 8), cross peaks between H14 and H6 support the substitution at C5 with the azo group, since substitution at C4 or C2 would preclude a close spatial arrangement of these protons. Cross peaks between H6 and H7a and H7b confirm their ortho-substituted relationship. The carbonyl carbons, C10 and C12, are assigned from the HMBC spectrum and have typical chemical shifts. The remaining OH protons attached to C2 and C4 are the broad signals at around δ 10 and 12, the chemical shifts being indicative of the presence of some form of hydrogen-bonding interactions.

The Relationship of Model Studies to the Role for Topa in the Active Site Chemistry of Copper Amine Oxidases. The overall reaction catalyzed by copper amine oxidases involves a two-electron oxidation of the amine substrate to aldehyde and ammonia, concomitant with the two-electron reduction of dioxygen to hydrogen peroxide (eq 1). Studies of several proteins of this class indicate a two-step ping-pong mechanism.[1] A complete model for topa quinone must therefore include a description of the role for cofactor in both the reductive (eq 7) and oxidative (eq 8) half-reactions:

$$E_{ox} + RCH_2NH_2 \rightarrow E_{red} + RCHO \quad (7)$$

$$E_{red} + O_2 \rightarrow E_{ox} + H_2O_2 + NH_4^+ \quad (8)$$

where E_{ox} contains topa in its oxidized, quino form (cf. $\mathbf{1}_{ox}$) and E_{red} contains topa in its reduced, aminophenol form (cf. $\mathbf{7H}_2$).[6,11]

A working mechanism for eq 7 has previously been proposed[6] and is summarized in Scheme IV. Basic features of this

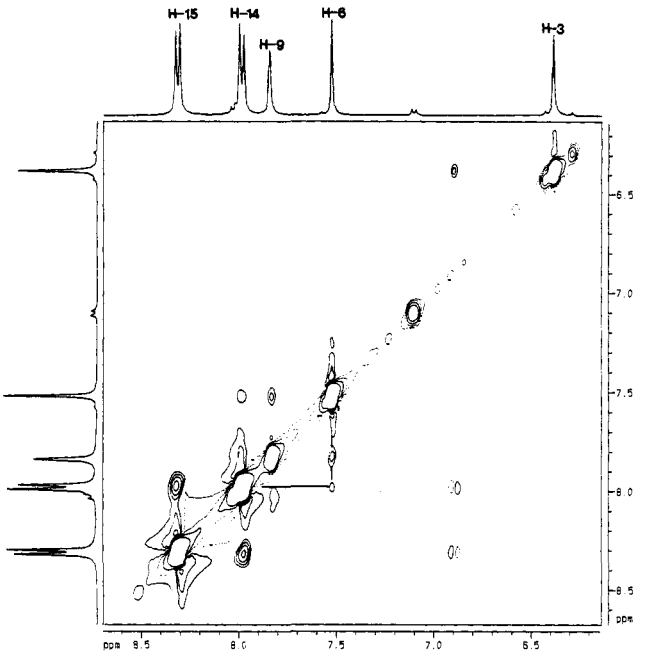

Figure 8. An expanded rotating-frame Overhauser enhancement (ROESY) spectrum of **3** at 400 MHz.

mechanism involve (i) the formation of a covalent adduct at the C5 position of the cofactor to form a substrate Schiff base complex, (ii) proton abstraction from C1 of the substrate by an active site base to yield a carbanion intermediate, which upon delocalization yields a reduced cofactor in a product Schiff base complex, and (iii) hydrolysis of the product Schiff base to release an aldehyde and generate the aminophenol of topa. Although the precise position of copper in the active site is not known, available data support its placement in proximity to the C2 oxygen of the cofactor.[14]

In the present study, a number of features of Scheme IV have been addressed, in particular the position of the cofactor undergoing attack by the substrate and the ionization state of the cofactor in the substrate and product Schiff base complexes. Earlier resonance Raman studies had shown identical spectra for hydrazone adducts of the model compound (**3**) and the active site, topa-containing peptide from bovine serum amine oxidase.[27] We therefore reasoned that demonstration of the position of attack of (4-nitrophenyl)hydrazine for the model compound would identify the position of the cofactor undergoing attack in the enzyme active site. The data in Figure 8 and Tables II and III show very clearly that hydrazone formation occurs at the C5 position of $\mathbf{1}_{ox}$, as anticipated for a *para*-quinone structure of hydroxyquinones. Experimentally, it has not been possible to conduct detailed structural studies of the complex formed between the substrate and cofactor. However, phenylhydrazines are known to be competitive inhibitors against substrate such as benzylamine.[19,28] This fact, together with the clear evidence for covalent adduct formation between benzylamine and the active site cofactor in several enzymes,[29,30] allows us to infer that the substrate forms a Schiff base complex at the C5 position of the topa cofactor.

In the course of reductive $NaCNBH_3$ inactivation experiments using [^{14}C]-benzylamine, [^3H]-$NaCNBH_3$, and either bovine serum amine oxidase[29] or the bacterial amine oxidase from *Arthrobacter P1*,[30] we have observed a quantitative incorporation of ^{14}C together with no incorporation of tritium. This result implicates reduction at the level of the substrate Schiff base

(27) Brown, D. E.; McGuirl, M. A.; Dooley, D. M.; Janes, S. M.; Mu, D.; Klinman, J. P. *J. Biol. Chem.* **1991**, *266*, 4049–4051.
(28) Rinaldi, A.; Floris, G.; Finazzi-Agro, A.; Giartosio, A.; Rotilio, G.; Mondovi, B. *Biochem. Biophys. Res. Commun.* **1983**, *115*, 841–848.
(29) Hartmann, C.; Klinman, J. P. *J. Biol. Chem.* **1987**, *262*, 962–965.
(30) Hartmann, C.; Klinman, J. P. *FEBS Lett.* **1990**, *261*, 441–444.

Scheme IV. Proposed Reaction Mechanism for the Oxidative Half-Reaction Catalyzed by Bovine Serum Amine Oxidase (ref 11)

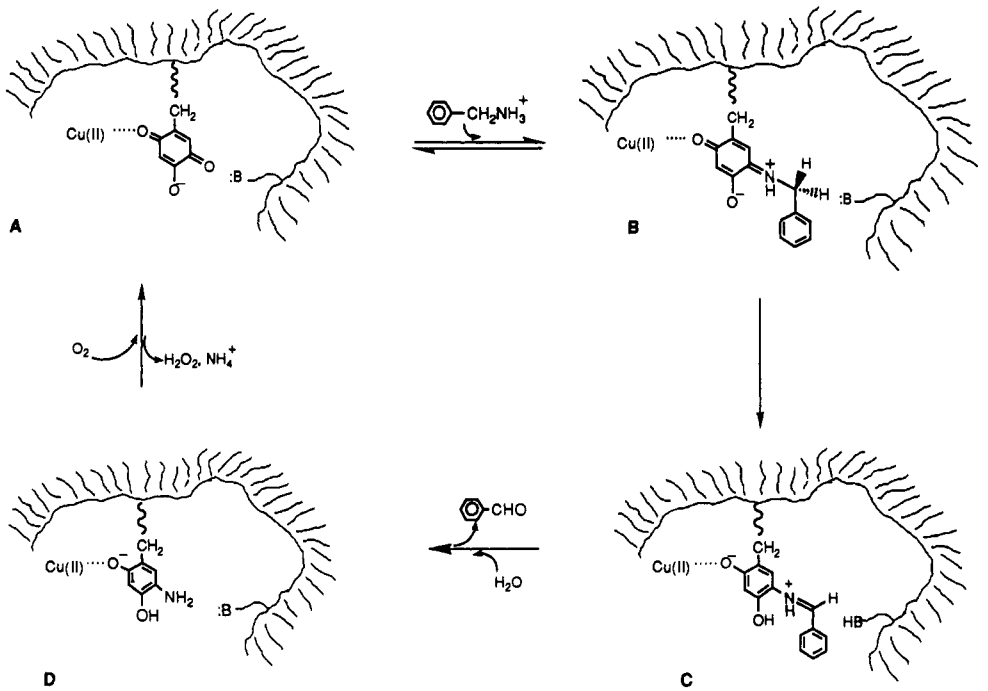

complex, since the intermediate formed in this case would be expected to labilize tritium into solvent:

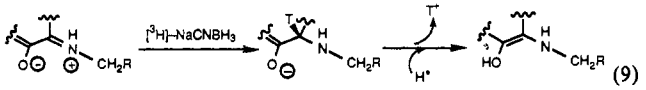

(9)

By contrast, the species formed from reduction of the product Schiff base complex is expected to incorporate tritium in a stable fashion:

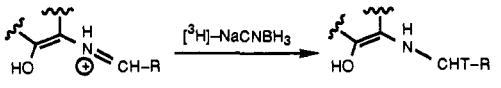

(10)

We conclude that the substrate Schiff base complex is characterized by a longer lifetime (accumulates to a significantly greater extent) than the analogous product Schiff base complex. This conclusion is fully supported by earlier studies of pH dependencies in the bovine serum amine oxidase reaction[31] and by the observation of extremely large deuterium[18] and tritium isotope effects in substrate oxidation.[32]

The results of the present study provide possible chemical insight into the differential stabilities of the substrate and product Schiff base complexes. As shown in Figure 1, the pK_a of the 4-hydroxyl group in topa quinone is quite low, with a value of 4.1 under our experimental conditions. Comparison of the enzyme to the model compound indicates an even lower pK_a of 3.0 (cf. Figure 2), which as already noted may reflect the proximity of cupric ion or a positively charged amino acid side chain. Given the high acidity of the oxidized cofactor, it is expected to remain ionized in both the initial structure and the resulting Schiff base complex with the substrate (A and B in Scheme IV). Stabilization of the substrate Schiff base complex should therefore occur readily via an electrostatic interaction between the cofactor oxyanion at C4 and a protonated Schiff base at C5.

Turning to the reduced cofactor, the data in Figures 3 and 4 show a significantly elevated pK_a, with pK_a values for the hydroxyl group of 9.17 ($\mathbf{1}_{red}H_3$) and 9.59 ($7H_2$). This indicates that reduction of the cofactor leads to an increase in pK_a of ca. 5 pH units, such that at physiologic pH values topa will be protonated. In an effort to incorporate a role for copper in our enzymatic mechanism, we have replaced one of the protons of the reduced cofactor by cupric ion (D, in Scheme IV). Analogous to species D, the precursor product Schiff base complex (C, Scheme IV) is expected to be protonated at C4. We therefore propose that uptake of a proton at this position is the origin of the reduced stability of the product Schiff base complex, leading to a loss of electrostatic stabilization by the neighboring oxyanion. In contrast to the short lifetime of the product Schiff base formed from benzylamine and the cofactor, recent rapid-scanning stopped-flow data[20] indicate a new absorbing species with 4-hydroxybenzylamine. This has been attributed to quinone methide formation:

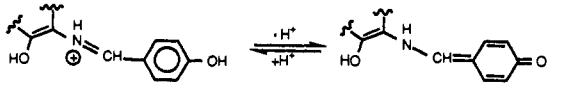

(11)

which stabilizes the product complex sufficiently that it can be observed under stopped-flow conditions.

We now address the oxidative half-reaction catalyzed by copper amine oxidases (eq 8) and the relationship of the data presented in this paper to this process. Although early studies had suggested an unchanged valence state for copper [as Cu(II)] throughout the catalytic cycle of copper amine oxidases, recent studies conducted by Dooley and co-workers under anaerobic conditions demonstrate an oxidation of reduced cofactor to a semiquinone species which is coupled to Cu(I) formation.[33] In light of these findings, a working mechanism for the oxidative half-reactions can be formulated, involving two sequential, one-electron oxidations (Scheme V). In the presence of dioxygen, this process presumably involves an intermediate $Cu(II)O_2^{\bullet-}$, which is expected to undergo very rapid reduction to $Cu(II)O_2H$. The electrochemical data reported in the present work indicate that topa undergoes a two-electron oxidation, without detection of semi-

(31) Farnum, M.; Palcic, M.; Klinman, J. P. *Biochemistry* **1986**, *25*, 1898–1904.

(32) Grant, K. L.; Klinman, J. P. *Biochemistry* **1989**, *28*, 6597–6605.

(33) Dooley, D. M.; McGuirl, M. A.; Brown, D. E.; Turowski, P. N.; McIntire, W. S.; Knowles, P. F. *Nature* **1991**, *349*, 262–264.

Scheme V. Proposed Mechanism for the Oxidative Half-Reaction Catalyzed by Bovine Serum Amine Oxidase (ref 33)

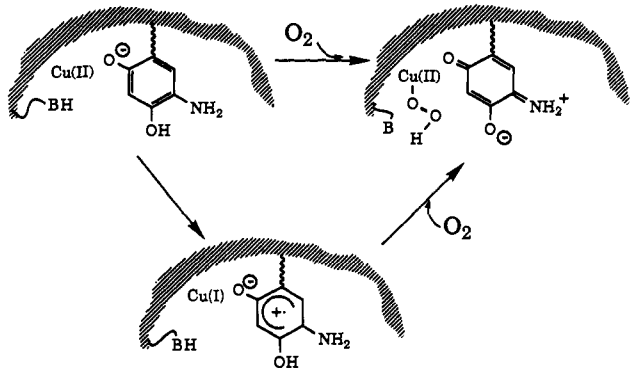

quinone species. Values for two-electron half-potentials as a function of pH are given in Figures 6 and 7 for topa (**1**) and dopa (**2**), respectively. It can be seen that at pH 7.2, the presence of the extra hydroxyl group in topa reduces the half-potential from 0.116 to −0.187 V *vs* SCE. With regard to the enzymatic mechanism, the more relevant half-potentials are those for aminophenol (**7**), which as shown in Table I display practically the same midpoint potentials as topa at pH 6.78 and 9.56. Thus, conclusions regarding the reducing capacity of topa can be generalized to the aminophenol form of the reduced cofactor. For the future it will be necessary to determine the redox potentials of protein-bound topa, to look for significant perturbations by active site copper and protein side chains. It will also be interesting to see if differences exist in redox capability among the varying copper amine oxidases. Nonetheless, it is of considerable interest that the redox potentials of topa and aminophenol are almost identical to values published previously for the dissociable quinocofactor PQQ.[23]

Finally, the data presented herein provide possible insight into the evolution of topa, rather than dopa, as the active site cofactor in copper amine oxidases. On the surface, dopa quinone would appear a more straightforward choice as the cofactor, given the prior existence of dopa as a naturally occurring amino acid. Additionally, free topa is know to be a highly unstable compound, with demonstrated neuro- and cytotoxic properties.[34] However, as the above discussion documents, the presence of the extra hydroxyl group in topa may play a key role in the action of copper amine oxidases. In the case of the reductive half-reaction (eq 7), the ionization state of the 4-hydroxy group is proposed to control the differential stabilities of the substrate and product Schiff base complexes. Turning to the oxidative half-reaction (eq 8), the extra hydroxyl group has a marked effect, increasing the reducing capacity of the quinone by 300 mV. We note that recent model studies have been successful in demonstrating amine oxidation with topa analogs; however, no activity has been observed with comparable dopa analogs.[35] It therefore appears that the simple introduction of a third hydroxyl group into dopa converts a catalytically inert species into a highly effective enzymatic prosthetic group.

Acknowledgment. We thank Dr. Graham Ball for running HMBC, HMQC, and ROESY NMR studies on **3** and his helpful discussions. We also thank Professor Marcin Majda for use of the instruments for the electrochemical study.

(34) Graham, D. G.; Tiffany, S. M.; Bell, W. R., Jr.; Gutknecht, W. F. *Mol. Pharmacol.* **1978**, *14*, 644–653.
(35) Mure, M.; Klinman, J. P. Unpublished results.